Computation of Radiation Heat Transfer in Aeroengine Combustors

NASA Grant NCC3-238

Submitted to

NASA Lewis Research Center

Final Technical Report

Grant Period: 11/ 22/ 1991 to 7/ 17/ 1996

S. V. Patankar

Principal Investigator
Professor of Mechanical Engineering
University of Minnesota
111 Church St. S. E.
Minneapolis, MN 55455

Introduction

In this report the highlights of the research completed for the NASA Grant #NCC3-238 are summarized. This research has been completed in the form of two Ph.D. theses by Chai (1994) and Parthasarathy (1996). Readers are referred to these theses for a complete details of the work and lists of references. In the following sections, first objectives of this research are introduced, then the finite-volume method for radiation heat transfer is described, and finally computations of radiative heat transfer in non-gray participating media is presented.

Objectives

Radiation heat transfer is a substantial portion of the energy transfer in many high temperature flow situations and we need efficient and accurate methods for its computation. The fluid flow and flow associated heat transfer analysis can be performed for such cases with existing Computational Fluid Dynamics (CFD) methods such as the control volume approach of Patankar (1980) . Over the past two decades, this method has merged as a popular fluid flow and heat transfer solution procedure. This method has been applied to simulate a variety of fluid flow and heat transfer processes that include electronic cooling, combustion chambers and green houses. Radiation can be an important heat transfer process in these applications. Therefore, it is desirable to employ a radiation heat transfer procedure that shares the same computational grid and philosophy with the control volume method. This approach eliminates the need to interpolate temperature, absorption coefficient, scattering coefficient and incident radiation during the iteration process. One of the objectives of this work is to develop one such radiation heat transfer procedure.

This procedure has to be validated against exact solution or other published benchmark solutions. Traditionally, validation of radiation numerical methods have been limited to a few simple cases for which exact solutions are available, or to those cases for which the Monte-Carlo method can provide solution easily. However, exact solution in radiation heat transfer are few, and Monte-Carlo solutions currently available in the literature are not useful as benchmark solutions. Hence, part of this work is devoted to developing benchmark solutions with the

Monte-Carlo method and testing the developed control volume procedure under different conditions.

One of the factors that complicates radiative heat transfer computations is the wavelength dependence of the properties of the media and surfaces, also called non-gray behavior. Such variation can be taken into account by "discretizing" the spectrum into bands, and assuming constant properties inside each band. The radiative problem can then be solved by solving for each band separately and adding the solutions. However, gases that constitute the participating media in combustion applications, have highly irregular absorption property variation with wavelength, characterized by many absorption lines within a small wavelength range. Procedure to treat the non-gray behavior of real gases are needed to model radiation heat transfer in real situation. Although work on non-gray gas modeling is not new, engineering models applicable to the Radiative Transfer Equation (RTE) solution-procedures are hard to find. The familiar narrow and wide band models average the spectral absorptance or transmittance of a column of gas over a wave-number range, hence predict path length dependent properties. since these do not provide absorption coefficient variation explicitly, they cannot be applied to the numerical TRE solution methods directly. Hence development of engineering non-gray gas models, applicable to any RTE solver, is important. Development of such models is another major objective of this work.

A Finite-Volume Method for Radiation Heat Transfer

In this part of the work, a radiation heat transfer calculation procedure for transparent, absorbing, emitting and scattering media was developed. The method solves the steady-state radiative transfer equation and employs the radiant intensity as the dependent variable. In this procedure , radiation direction is allowed to vary within a control angle, while the magnitude of the radiant intensity is assumed constant within the same control angle. It is applicable for transport (non-participating) as well as participating media.

This method shares the same computational grid with some available control volume procedures used in CFD and is developed for both Cartesian and general

body-fitted curvilinear-coordinates. In the Cartesian coordinate system, irregular geometries are modeled using an extension of the blocked-off region

procedure of Patankar (1980). Figure 1 shows the applications of a blocked-off region and curvilinear non-orthogonal grids to simple and complex irregular geometries. Both the blocked-off region approach and the body-fitted curvilinear-coordinates formulations were extended to three dimensions.

It was shown that by tracing the radiant intensity to an upstream location and by using an exponential-type scheme, more accurate solutions are obtained. However, additional computer storage and run time are needed for this added accuracy. As a result, the step scheme is used in general curvilinear coordinates. It should be mentioned that the more complex approach should produce more accurate solution for a given spatial and angular discretization.

During the development of this procedure, various aspects of the discrete ordinates method and finite-volume method were examined. As a result of this examination, a linearized equation of transfer and a modified-exponential scheme were proposed. The source-term linearization practice of Patankar (1980) was used in the formulation of the linearized equation of transfer.

Various test problems were used to test the procedure presented in this work. These problems range from transparent to anisotropically scattering media, tow- and three-dimensional, black and gray enclosures with diffuse and collimated incidence. Based on the results of these tests, the finite-volume method is a viable numerical radiative heat transfer procedure.

Test problem 1

Figure 2 shows a curved irregular geometry studied by Chai (1994) and Parthasarathy (1996) using a Monte-Carlo method. This problem consist of a quarter of a circle with a rectangular region added at the top. The outer wall of the circle is hot, while the remaining walls and the medium are cold. The medium absorbs and scatters energy anisotropically with an extinction coefficient of 1 m^{-1}. Figure 3 shows samples blocked-off region and body-fitted coordinates grids for the chosen problem.

Figures 4, 5, and 6 show the heat flux distributions at the top wall for the isotropic, F1, and B1 scattering phase functions respectively. The solution compare

very well with the Monte-Carlo solutions. Figures 7 and 8 show the heat flux distributions at the right wall for the F2 and B2 scattering phase functions respectively. Accurate solution were also obtained. Figure 9 shows the right wall heat fluxes for transparent, purely absorbing, and anisotropically scattering media. Solution obtained with Monte-Carlo method, the blocked-off region grid, and the body-fitted coordinates procedures agree with each very well.

Test problem 2

Figure 10a and 10b show the computational grid for a furnace enclosure for the blocked-off and body-fitted coordinates procedures. Sample solutions for a pure radiation problem obtained using these grids are shown in Figure 10c. The wall temperatures are as shown in Figure 10b. The volumetric heat generation in the medium is 5 kW/m^3, and the absorption coefficient of the medium is taken as $1m^{-1}$. Figure 10c shows the heat flux on the front wall of the furnace at three different heights for a non-scattering medium. It can be seen that the Cartesian coordinates blocked-off region procedure and the body-fitted coordinates procedure produce comparable results.

Computation of Radiative Heat Transfer in Non-Gray Participating Media

Consistent with the goals of the research, non-gray gas modeling was taken up as the next major objective. The requirements for a non-gray model were that it should be independent of path-length correlations and be applicable to the finite volume procedure developed for a gray medium, without major modifications. For this reason, band models which predict transmissivity or band absorptance for a certain path length cannot be directly used. The k-distribution method, the weighted-sum-of-gray-gases (WSGG) method, and other methods with similar concepts provide the absorption coefficient explicitly and are suitable to the numerical procedures used to solve the RTE. Three such procedures were formulated and tested.

In the k-distribution method, integration over wave-number for a total quantity is replaced by integration over the absorption coefficient (κ) for a narrow wave-number range. This is done with the help of the absorption coefficient frequency distribution function, or $f(\kappa)$. This is economical considering the rapid

and irregular variation of absorption coefficient of a gas. Analytical expressions for the frequency distribution function $f(\kappa)$ can also be found as the inverse Laplace transform of the narrow band transmissivity. In place of $f(\kappa)$, the cumulative distribution function $g(\kappa)$ may also be used, which is equivalent to reordering the absorption coefficient values according to their strengths, rather than their positions in the narrow wave-number interval. $g(\kappa)$ is a monotonic function of κ and can be inverted to find $\kappa(g)$. A procedure to model non-gray gas radiation based on this method was formulated, with the help of the analytical expressions for $f(\kappa)$ and narrow band model parameters. This is denoted as narrow band k-distribution (KD-NB) model in this document. In each of the narrow wave-number intervals (25-50 cm^{-1}), the smooth absorption coefficient distribution $\kappa(g)$ is divided into the desired number of sections and the RTE is solved for each of these.

Although the narrow band k-distribution method is accurate and more efficient than the line-by-line approach, it is still time-consuming because of its narrow band nature. The concept of reordering the absorption coefficient spectrum to obtain a smooth function can be extended to the whole vibration-rotation band. For a wide band, the reordering can be obtained from a wide band model absorptance function. An analytical expression for the wide band $f(\kappa)$ function (similar to the k-distribution function) was obtained, making the procedure very simple. With the help of wide band parameters, the reordering could be obtained for all bands of a gas. Each band is then divided into an appropriate number of sections, and the RTE solved for each section. This approach is termed the wide band k-distribution (KD-WB) method here. The blackbody intensity, and the properties of boundaries and particulates have to be assumed constant in the interval of a gas band. Hence this approach cannot accommodate arbitrarily varying boundary or particulate properties. The KD-WB is faster than the KD-NB but the solution is less accurate. Moreover, since the location of the vibration-rotation bands are fixed, other slowly-varying non-gray properties are difficult to accommodate.

The third approach called the KD-WSGG method, is a combination of the KD-NB and the WSGG methods and was formulated in order to accommodate non-gray boundaries and particulates. In the WSGG method, the absorption coefficient range is divided into a number of 'gray gases' or $\Delta\kappa$ intervals. An appropriate weight for each gray gas is determined as the fraction of the blackbody

intensity in the regions where the absorption coefficient is in the range $\Delta\kappa$. The cumulative k-distribution $g(\kappa)$ can be used to weight the Planck's function in each narrow band for each gray gas, and summed with similar quantities from other narrow bands, to find the gray gas weights for the entire spectrum. Since the narrow bands of the KD-NB method are narrow relative to the scale of variation of particulate or boundary properties, the spectrum can be divided into bands based on these properties. In each of these wide bands, the above procedure of finding gray gas weights can be applied. The RTE is solved for each gray gas in each band, and the results summed. This method is computationally the most efficient since it combines blackbody intensities for similar absorption coefficients. Other non-gray properties of the system can also be taken into account by this approach.

The non-gray approaches were validated by comparing their solutions with other published solutions. The performance of these approaches to solve non-gray radiation problems with in-homogeneous media in complex multidimensional geometries were also examined.

Test problem 3

Here the solution for a three-dimensional complex geometry shown in Figure 11 is presented. The geometry represents a typical coal-fired power-plant boiler. The dimensions of the furnace and spatial grid is shown in the two-dimensional views at $z = z_{max}$ and $x = 0$ in Figure 12. A homogeneous medium of 50% water vapor was assumed for the problem and temperature varies only in the y-direction.

The RTE is solved with the body-fitted coordinates formulation of the finite volume method. Thirty gray gases were used for the non-gray gas modeling with the KD-WSGG approach. The spatial and angular grids used were 10x40x10 and 16x8 respectively. The radiative dissipations at some cross sections of the geometry are shown. Figure 13 represents the radiative dissipation contours predicted for the x-y plane at z=4.015 m. The large gradient of radiative flux towards the limits of the rectangular region is due to the jump from 1500 K to lower temperatures. The lower temperature gas elements here absorb more than they emit, and contribute to positive values in radiative energy dissipation. Also, the concentration of the lines near the walls is due to the large temperature

gradients. Similar trends are observed in the z-y plane at x = 4.015 m and are shown in Figure 14.

Figure 15 shows the heat flux on the front wall of the furnace at x = 4.015 m, plotted against the vertical distance y. Heat flux to the wall increases from the bottom for the first trapezoidal section, as the wall sees more of the hotter gas as y increases. The inflection point around 4m is due to the jump in gas and wall temperatures. The maximum heat flux is around the middle portion of the vertical wall, which has the highest view factor to the emitting surfaces and medium. Figure 16 shows the heat flux on the same wall at three different y-locations, plotted as a function of x. The heat flux naturally decreases at the corners, which have smaller views of the hotter gas. As is shown in Figure 15, the heat flux is highest around the middle (y=10.825 m), lowest at the y=5 m.

REFERENCES

Chai, J. C., 1994, "A finite Volume Method for Radiation Heat Transfer," Ph.D. thesis, University of Minnesota.

Parthasarathy, G., 1996, "Computation of Radiative Heat Transfer in Non-Gray Participating Media" Ph.D. thesis, University of Minnesota.

Patankar, S. V., 1980, *Numerical Heat Transfer and Fluid Flow* , Hemisphere Publishing, New York.

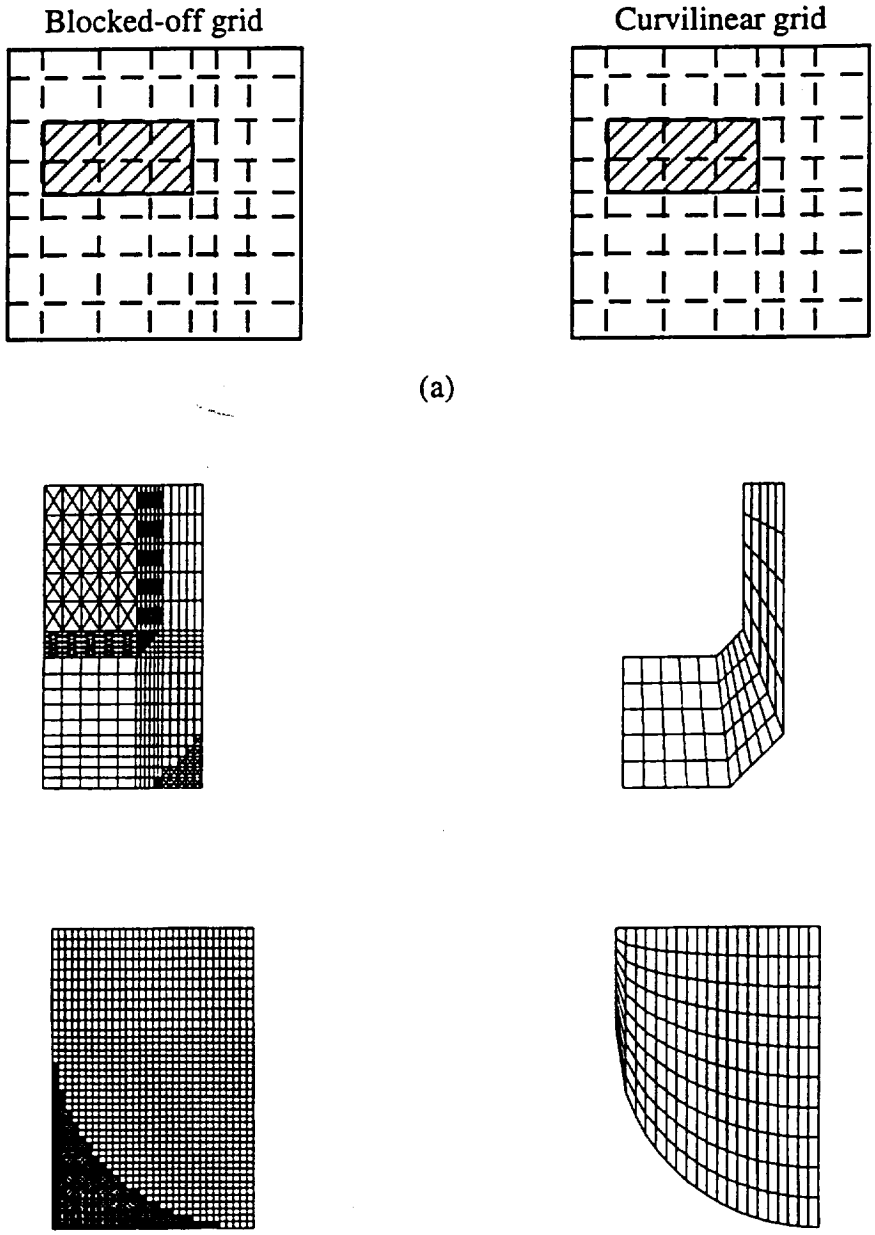

Figure 1 The blocked-off region and curvilinear grids; (a) Simple and (b) Complex irregular geometries

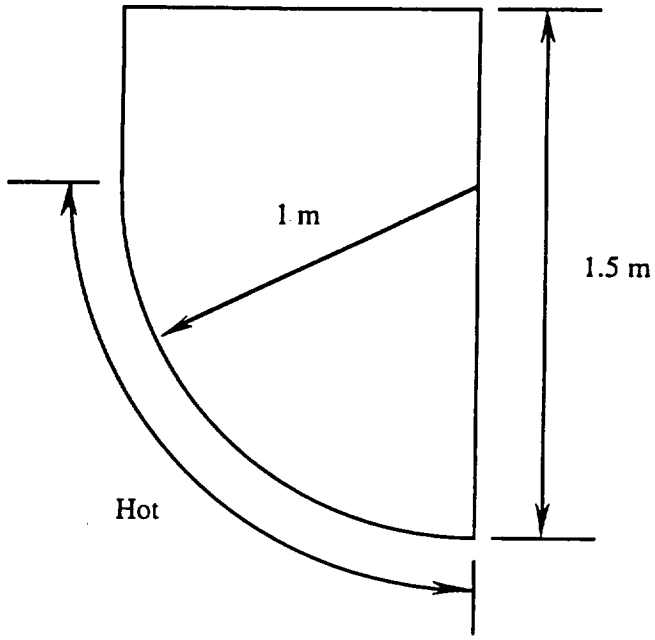

Figure 2 Schematic of a curved irregular geometry

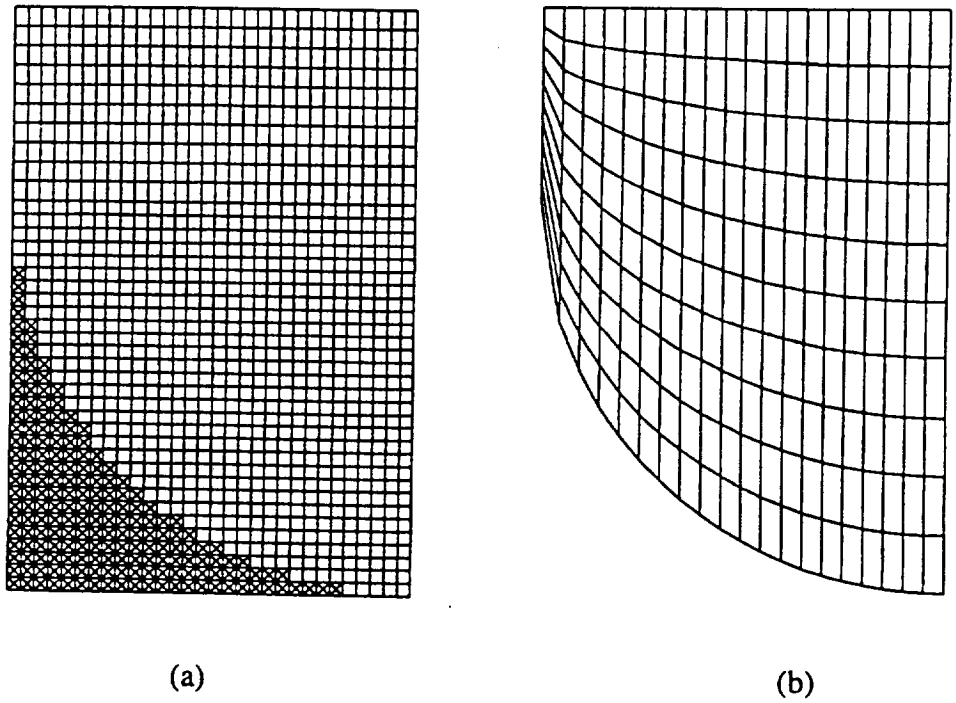

Figure 3 Sample spatial computational grids; (a) Blocked-off region procedure, (b) body-fitted coordinates procedure

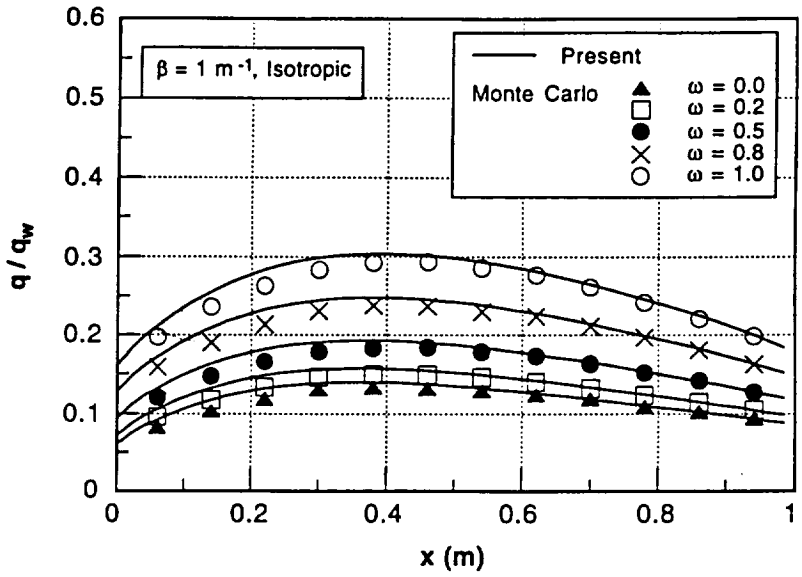

Figure 4 Heat Flux distributions along the top wall

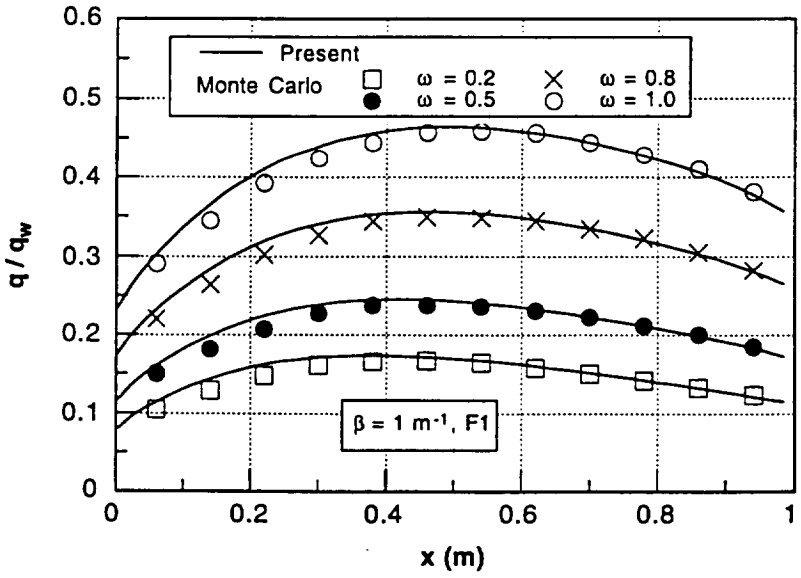

Figure 5 Heat Flux distributions along the top wall

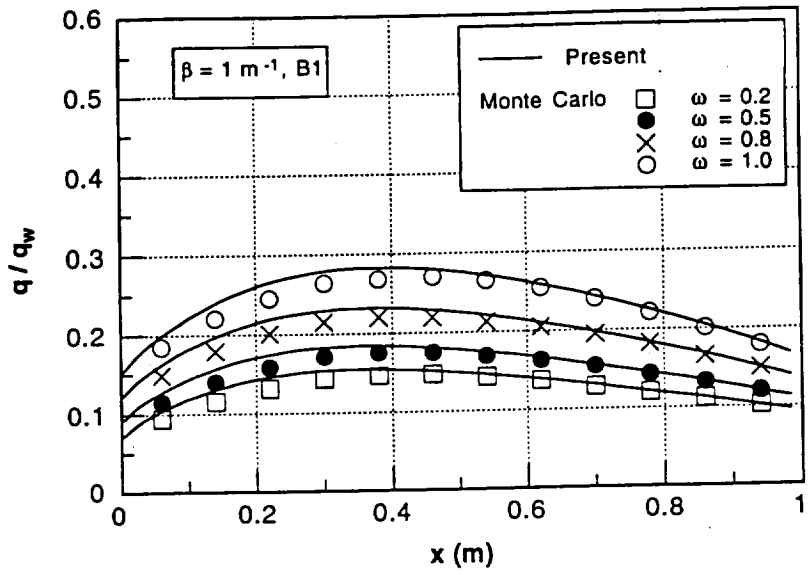

Figure 6 Heat Flux distributions along the top wall

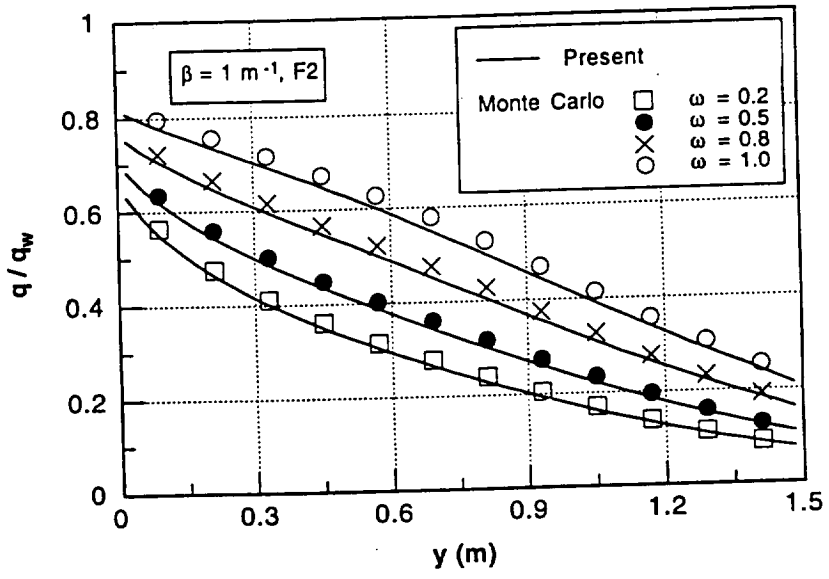

Figure 7 Heat Flux distributions along the right wall

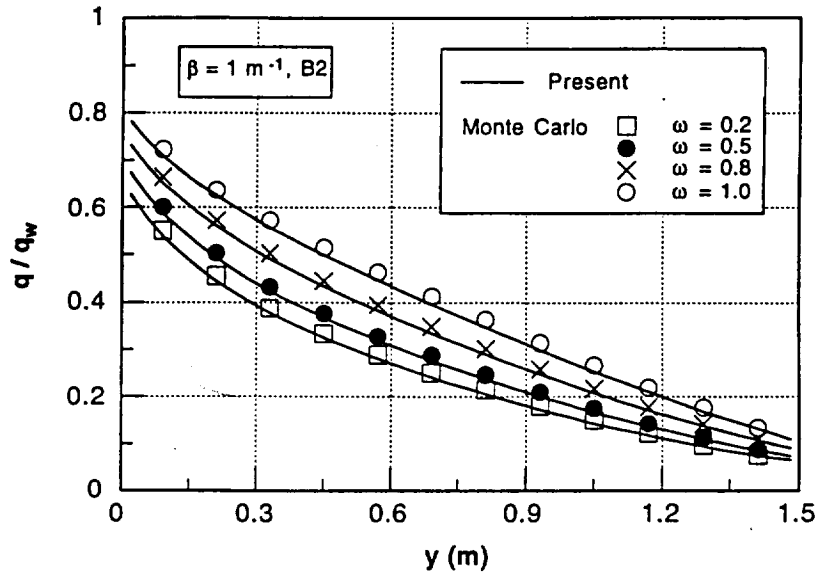

Figure 8 Heat Flux distributions along the right wall

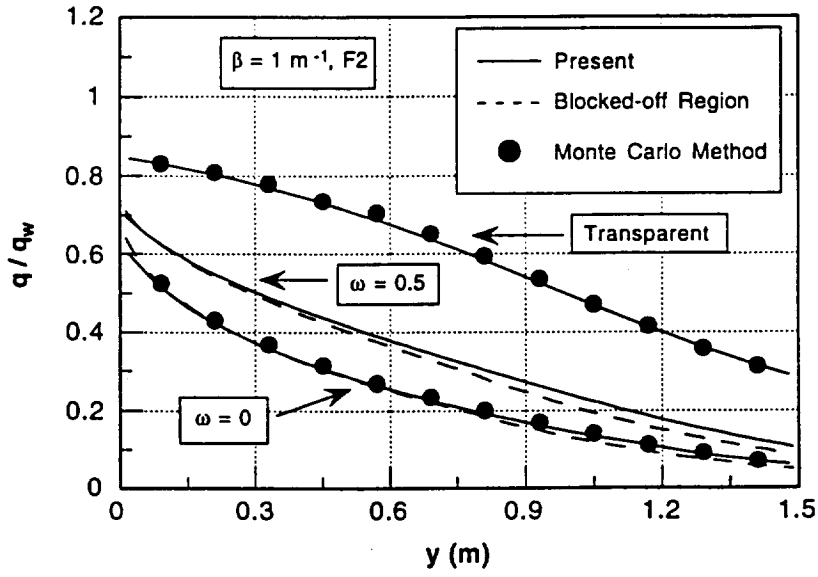

Figure 9 Heat Flux distributions along the right wall

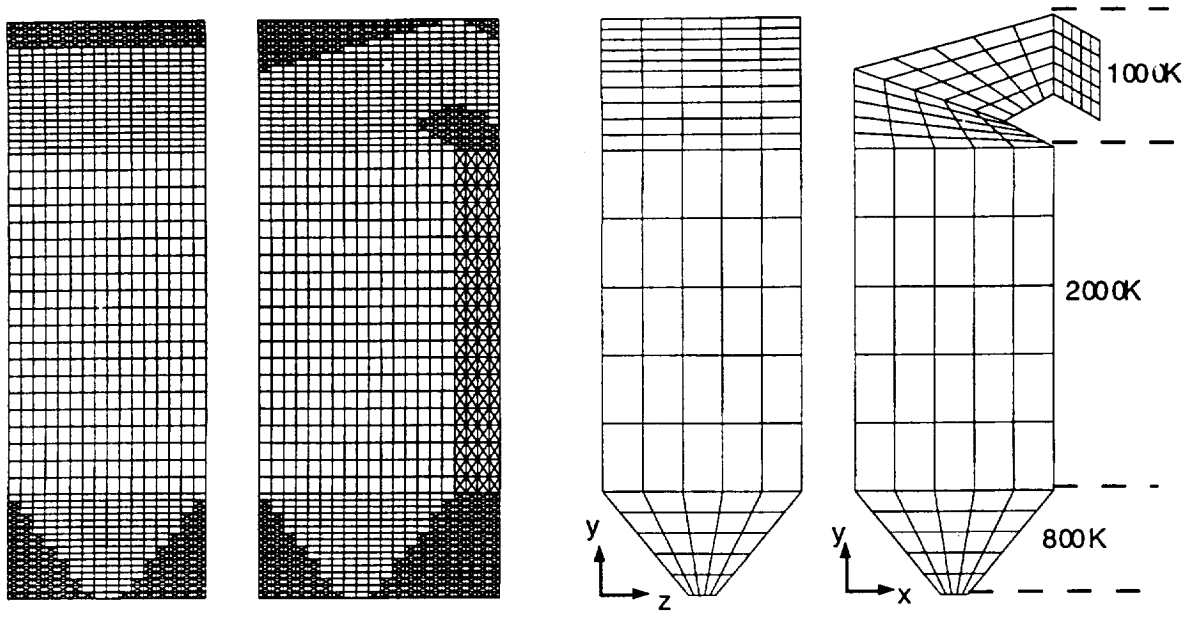

(a) (b)

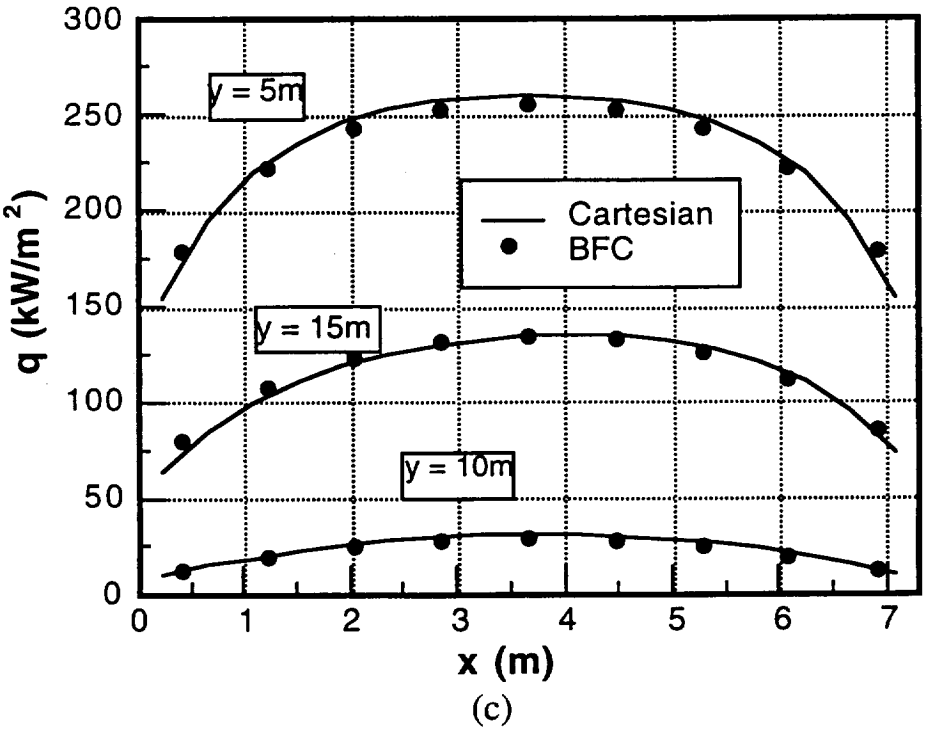

(c)

Figure 10. Computational grid for the blocked off region procedure (a) and the curvilinear coordinates procedure (b), and the computed heat flux on the front wall (z=0).

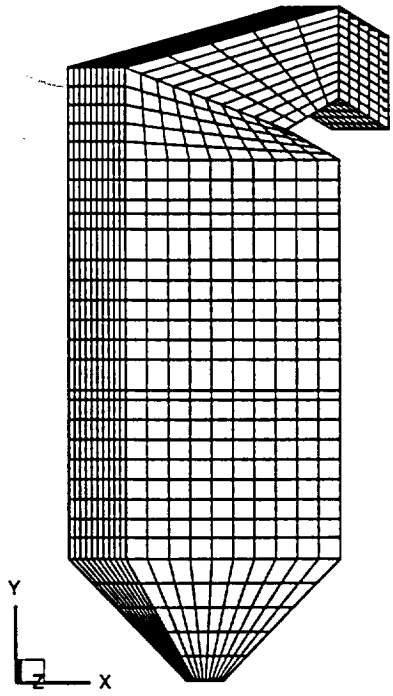

Figure 11 Furnace model

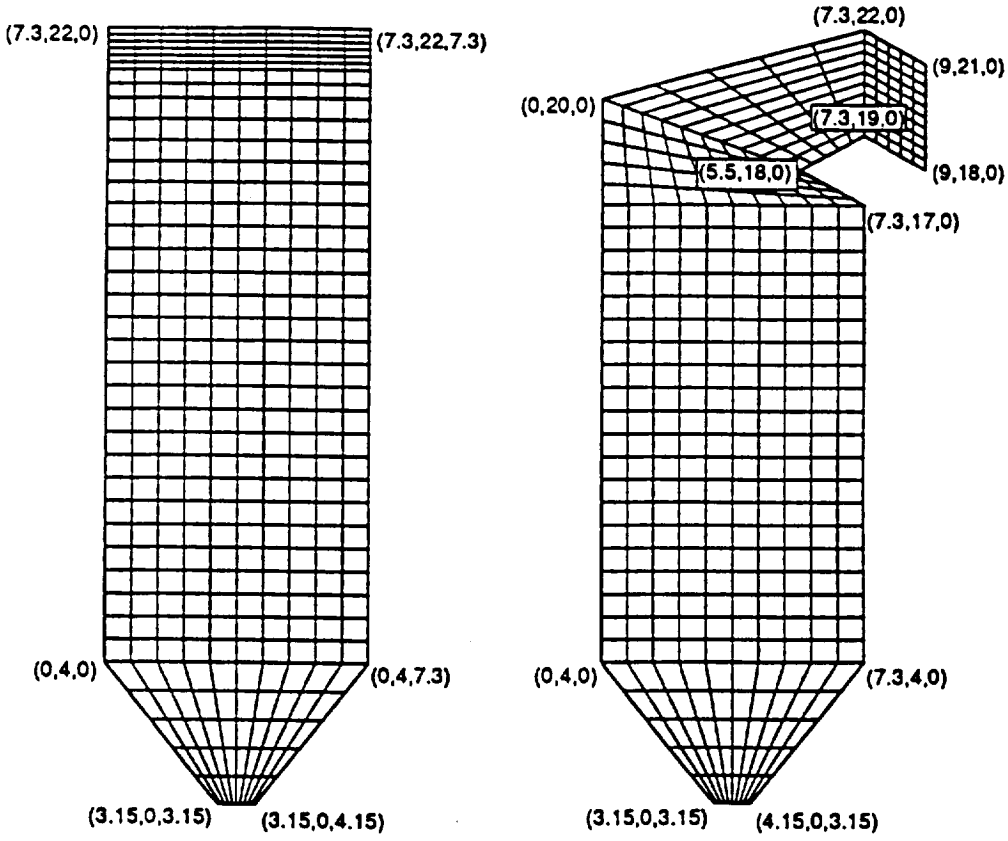

Figure 12 Furnace dimensions and sample mesh

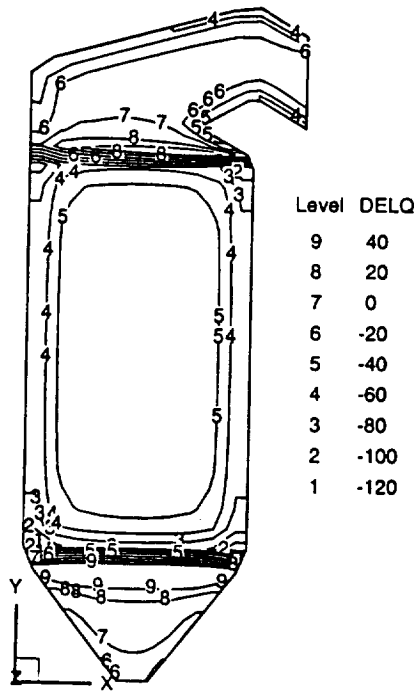

Figure 13 Radiative dissipation contours at z = 4.015 m plane

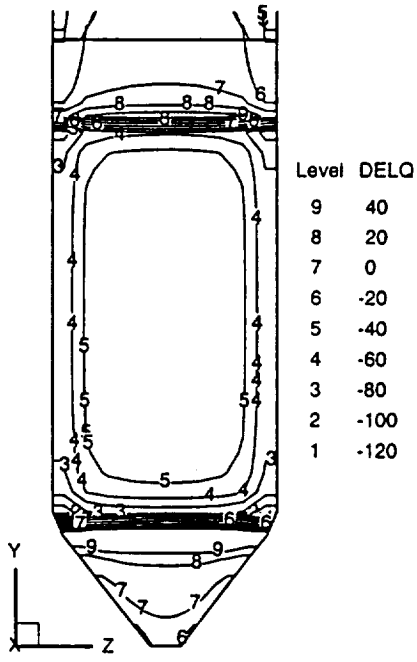

Figure 14 Radiative dissipation contours at x = 4.015 m plane

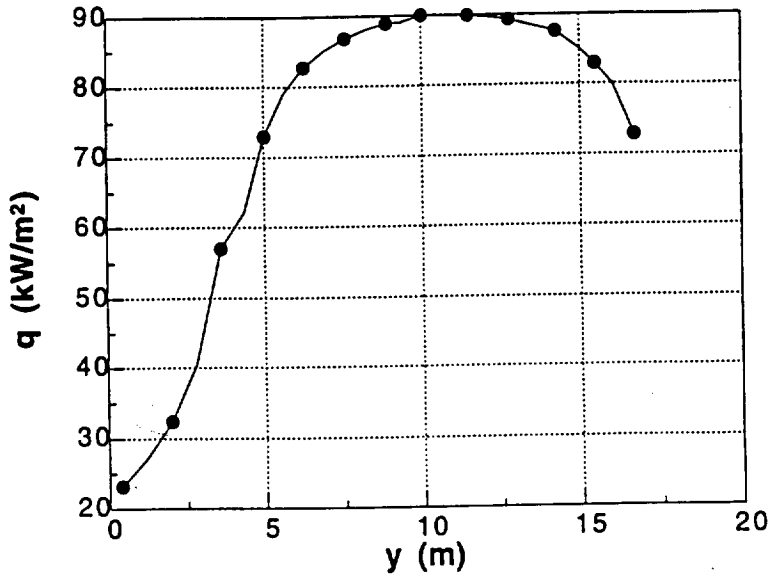

Figure 15 Radiative heat flux distribution on the front wall at x = 4.015 m

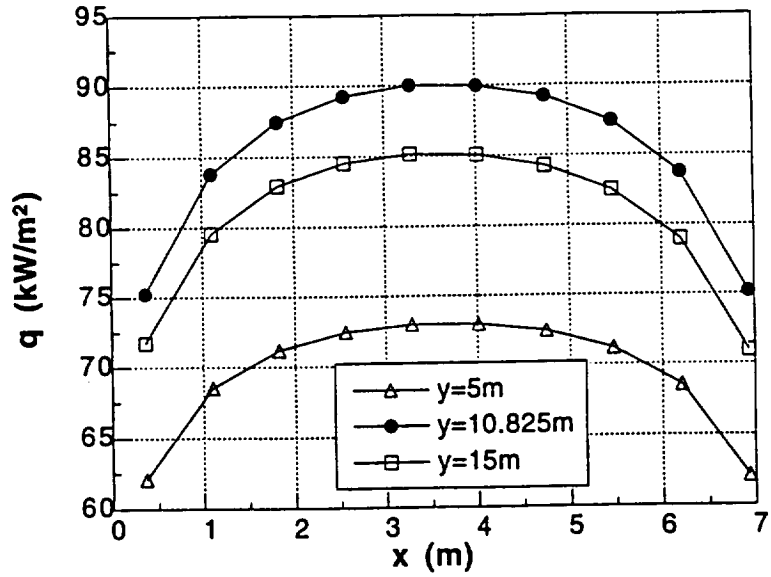

Figure 15 Radiative heat flux on the front wall at different heights